EUROFUSION WPHCD-PR(16) 16310

P Kalaria et al.

RF Behavior and Launcher Design for a Fast Frequency Step-tunable 236 GHz Gyrotron for DEMO

Preprint of Paper to be submitted for publication in
Frequenz-Journal of RF-Engineering and Telecommunications

This work has been carried out within the framework of the EUROfusion Consortium and has received funding from the Euratom research and training programme 2014-2018 under grant agreement No 633053. The views and opinions expressed herein do not necessarily reflect those of the European Commission.

RF Behavior and Launcher Design for a Fast Frequency Step-tunable 236 GHz Gyrotron for DEMO

P. C. Kalaria[1], K. A. Avramidis[1], J. Franck[1], G. Gantenbein[1], S. Illy[1], J. Jin[1], I. Gr. Pagonakis[1],
M. Thumm[1,2] and J. Jelonnek[1,2]
[1]Institute for Pulsed Power and Microwave Technology (IHM),
[2]Institute of Radio Frequency Engineering and Electronics (IHE)
Karlsruhe Institute of Technology (KIT)
Karlsruhe, Germany

Abstract— **As part of the EUROfusion project, the conceptual design of a 1 MW 236 GHz hollow-cavity gyrotron is ongoing at IHM, KIT for a DEMOnstration Power Plant (DEMO), along with a 2 MW coaxial-cavity design concept. Fast frequency-tunable gyrotrons (tuning within a few seconds) are recommended for plasma stabilization using a non-steerable antenna. In this work, the mode-selection approach for such a frequency-tunable gyrotron is presented and suitable operating modes for fast frequency tunability are suggested. Magnetic field tuning has been studied as an effective technique to tune the gyrotron operating frequency. The step-tunability of the 236 GHz gyrotron within the frequency range of ±10 GHz in steps of 2-3 GHz is demonstrated in numerical simulations. A hybrid-type Quasi-Optical Launcher (QOL) has been designed for a step-frequency tunable gyrotron with sufficiently high Fundamental Gaussian Mode Content (FGMC).**

Keywords— DEMO; frequency tunability; gyrotron; plasma instabilities control; tokamak; quasi-optical launcher

I. INTRODUCTION

Gyrotron oscillators (gyrotrons) are extensively used sub-millimeter and millimeter wave sources with a wide range of applications, such as material processing, high-resolution spectroscopy, radars, etc. [1]. However, the main applications of high-power (~ 1 MW), high-frequency (100 GHz – 300 GHz) gyrotrons are plasma start-up, Electron Cyclotron Resonance Heating (ECRH), non-inductive current drive and plasma stability control in plasma experiments relevant for nuclear fusion research. For example, for the Wendelstein 7-X (W7-X) stellarator in Greifswald (Germany), in total ten 140 GHz, 1 MW CW (1800 s) hollow-cavity gyrotrons are completely installed to fulfill the total ECRH requirement [2]. In the ITER tokamak, 24 gyrotrons with an operating frequency of 170 GHz are planned for a total power requirement of 20 MW [3-5]. After ITER, first prototypes of a fusion power plant are foreseen, termed DEMOnstration power plants (DEMO) [6]. According to the European Union 2012 baseline of DEMO (aspect ratio of 4.0), the detailed design goals for gyrotron development are listed in Table I [7-10], together with technological constraints. This baseline has been updated in 2015 to the 2015 EU DEMO1 Baseline, involving an aspect ratio of 3.1 [11]. As a consequence, lower frequencies of around 170 GHz and 200 GHz are now considered to be more relevant. Although the present study targets 236 GHz, the conclusions on frequency step-tunability can be readily transferred to lower frequencies. In addition, the presented gyrotron design has been developed in a way to have the capability of comparable operation also at the lower frequencies of interest [12].

TABLE I. DESIGN GOALS AND TECHNOLOGICAL CONSTRAINTS FOR DEMO GYROTRONS [7-8].

Goals	
Main frequency	230 – 240 GHz
Output power	~ 1 – 2 MW
Overall efficiency (with multi-stage depressed collector)	> 60%
Interaction efficiency	> 35%
Frequency step for fast tunability	2 – 3 GHz
Frequency step for (slow) multi-frequency operation	30 – 40 GHz
Constraints	
Peak ohmic wall loading at cavity	≤ 2 kW/cm^2
Emitter current density	≤ 4 A/cm^2
Electric field at emitter (cathode)	≤ 7 kV/mm
Spread of electron guiding centers in cavity	≲ λ/5
Emitter radius	~ 50 – 70 mm

Under normal conditions, tokamak plasmas are toroidally symmetric and all field lines on a particular magnetic flux surface carry the same current. In the case of tokamaks with high plasma density, radiation cooling at the edge and plasma transport processes increase the plasma current. This increased plasma current, also known as ‘Bootstrap current’, flows along the magnetic lines which causes corrugations in the magnetic flux surface and generates magnetic islands. This condition reduces pressure inside the plasma and consequently reduces fusion energy. The bootstrap current is proportional to the pressure gradient, so it is removed from magnetic islands. The reduction of bootstrap current further increases the size of the

---

This work has been carried out within the framework of the EUROfusion Consortium and has received funding from the Euratom research and training programme 2014-2018 under grant agreement No 633053. The views and opinions expressed herein do not necessarily reflect those of the European Commission. Parts of the simulations presented in this work have been carried out using the HELIOS supercomputer at IFERC-CSC.

magnetic islands. The resulting large magnetic islands increase the toroidal transport which is called a neoclassical tearing mode (NTM) that leads to major loss of confinement and disruption [13-14]. This type of instability can be avoided by driving current in the magnetic island. Electron Cyclotron Current Drive (ECCD) is the preferred method for NTM stabilization due to its precise localization of the power deposition [15-16].

The location of such instabilities inside the plasma is not fixed, which demands steerable RF beams for complete control. For plasma stabilization in smaller experiments, mechanically steerable mirrors have been used to direct the EC millimeter waves to the particular positions. However, movable parts are then close to the plasma, which requires flexible cooling pipes. Because of high thermal and neutron fluxes, this method is not preferable for fusion reactors. The condition for resonanace RF absorption can be described as $\omega - k_z v_z = \Omega$ (where ω = angular frequency of the RF wave, k_z = z-component of the wave number, v_z = electron velocity along z-direction and Ω = electron cyclotron frequency). Due to the large plasma volume in advanced magnetic confinement fusion experiments and fusion reactors, the magnetic field varies significantly from the plasma center to its edge. Hence, the resonance condition between cycling electrons in the plasma and millimeter waves of a certain frequency is fulfilled in a small plasma layer. Therefore, it is useful to have fast-frequency-tunable gyrotrons as ECRH sources, which allows to control the plasma instabilities employing fixed launching mirrors [17-18].

The operating frequency of a gyrotron is close to the gyrofrequency of the electrons or its harmonics, see Eq. 1, where, B_0 is the magnetic field at the cavity center, s is the harmonics number, m_e is the electron rest mass, γ is the relativistic Lorentz factor and U is the acceleration voltage. From Eq. 1 and 2, it is clear that the gyrotron operating frequency is highly dependent on the cavity magnetic field, while it is weakly dependent on the beam energy through the relativistic factor. Consequently, magnetic field tuning is a very effective way to change the operating frequency of high-power gyrotrons.

$$f \approx \frac{e \cdot B_0}{2\pi \cdot s \cdot m_e \cdot \gamma} \Rightarrow f \approx \frac{28\ \text{GHz}}{s} \cdot \frac{B_0(\text{T})}{\gamma} \tag{1}$$

$$\gamma = 1 + \frac{eU}{511\ \text{keV}} \tag{2}$$

The minimum time needed for switching the operating frequency is then determined by the growth rate of possible magneto-hydrodynamic instabilities in the fusion plasma. Large fusion experiments require frequency changes of several GHz/s. For plasma stabilization, one can achieve fast gyrotron frequency tunability in a limited frequency range only by adjusting the gyrotron magnetic field with auxiliary solenoids, keeping the magnetic field by the main solenoid constant. The configuration of a realistic 10.5 T superconducting magnet for the DEMO gyrotron is under investigation at IHM, KIT [19].

Apart from an advanced magnet design, a broadband output window is necessary for a frequency-tunable gyrotron. The transmission properties of conventional single-disk windows allow gyrotrons only having operating frequencies $f_N = (c/2 \cdot d \cdot \sqrt{\varepsilon_r}) \cdot N \ = f_1 \cdot N$ within ± 1 GHz. Here, d is window thickness, ε_r is the relative permittivity of the material and N is an integer number. For standard window thicknesses (1.50 mm to 2.25 mm) of CVD-diamond windows ($\varepsilon_r = 5.67$), the corresponding basic frequency (f_1) is between 42 GHz and 28 GHz, which does not support step-frequency tunability [20]. The Brewster window, which has a wide transmission band is a favorable option for frequency step-tunability. Its development and corresponding experiments at KIT are reported in [21-22].

In this paper, a feasibility study of a fast-frequency tunable, hollow-cavity 236 GHz DEMO gyrotron is presented. The basic principles behind mode selection for a frequency-tunable high-power gyrotron are explained in Section II. The finalized cavity design and its frequency tunability are discussed in Section III and the results of launcher design are presented in Section IV. The in-house code packages “EURIDICE” [23], “CAVITY” [24] and “TWLDO” [33] have been used for the simulations. It should also be noted that at KIT, along with the hollow-cavity design, the conceptual design of a 2 MW coaxial-cavity DEMO gyrotron and the development of an advanced gyrotron test facility are also ongoing [25].

II. MODE SELECTION APPROACH FOR THE FREQUENCY-TUNABLE GYROTRON

At frequencies around 236 GHz, a very high order TE_{mn} mode (eigenvalue χ_{mn} > 100) has to be used as the operating mode in the gyrotron cavity to reduce wall loading and to achieve sufficiently high output power of around 1 MW. As discussed in [25], the co-rotating mode $TE_{43,15}$ has been

TABLE II. SUITABLE OPERATING MODES AND THEIR PROPERTIES FOR A FAST-FREQUENCY TUNABLE, HOLLOW-CAVITY GYROTRON WITH BROADBAND BREWSTER WINDOW. FREQUENCY STEPS: Δf = 2 - 3 GHz.

Frequency [GHz]	**227.4**	**230.3**	**233.1**	**236.0**	**238.9**	**241.8**	**243.9**
Δf [GHz]	2.9	2.8	2.9	-	2.9	2.9	2.0
Cavity TE mode (indices *m*,*n*)	40,15	41,15	42,15	43,15	44,15	45,15	43,16
Relative caustic radius ($R_{caustic}/R_{cav}$)	0.402	0.407	0.412	0.417	0.421	0.427	0.403
Electron beam radius (r_b)	8.77	8.87	8.97	9.06	9.16	9.26	8.78

selected for the 236 GHz hollow-cavity gyrotron, which continues the mode series given in [26]. The relative caustic radius ($R_{\text{caustic}}/R_{\text{cav}} = m/\chi_{mn}$) of the $TE_{43,15}$ mode is 0.417 and the cavity radius $[R_{\text{cav}} = (c \cdot \chi_{\text{mn}})/(2\pi \cdot f)]$ is 20.88 mm. Here, m is the azimuthal mode index, χ_{mn} is the n-th root of the derivative of the Bessel function J_m and c is the speed of light. The selected operating modes for the frequency tunability must fulfill the following criteria:

a) For the chosen cavity radius, the mode eigenvalues must correspond to frequencies in the desired frequency band.

b) The coupling to the electron beam has to be large for all modes, especially compared to possible competitors.

c) The functionality of the output launcher and of the mirror system decreases if the caustic radius of the operating mode differs from the design caustic. Therefore, the caustic radii of the modes have to be as close as possible.

In the present design, the modes selected for frequency step-tuning within the range of −10 GHz to +10 GHz around 236 GHz (mode $TE_{43,15}$) are listed in Table II. With these proposed modes, the maximum relative caustic radius deviation is only 3.5 % from the average value, which ensures that the same optimized quasi-optical launcher and optical system design works for all modes with only very small radial shift of the Gaussian RF output beams. Apparently, frequency tunability in steps of 2-3 GHz can be achieved in the case of the 236 GHz hollow-cavity gyrotron.

The most suitable electron beam radius r_b for an individual co-rotating (−) or counter-rotating (+) mode can be calculated using $r_{\text{b}} = (\chi_{m\mp1,1} \cdot R_{\text{cav}})/\chi_{mn}$ [27]. The mode spectrum around the $TE_{43,15}$ mode, assuming a beam radius of 9.06 mm, is presented in Fig. 1. All neighboring modes within the frequency range of 224 GHz to 260 GHz having relative coupling higher than 0.35 (with respect to $TE_{43,15}$) are considered and the selected operating modes are marked in Fig. 1. Of course, the relative couplings change with the beam radius; and for each mode, the r_b value given in Table II is an optimized value.

III. FREQUENCY TUNABILITY OF THE DEMO GYROTRON

The hollow-cavity design for the 236 GHz DEMO gyrotron and its RF behavior have been discussed in detail in [9] [12] [28]. The designed cavity with the longitudinal field profile of the $TE_{43,15}$ mode is shown in Fig. 2 and the values of all geometric parameters are listed in Table III. As a next step, the frequency tunability of the proposed cavity has been verified with all selected modes. The operating parameters of the gyrotron (beam energy and magnetic field) have been optimized by considering a constant beam current of 43 A and a minimum interaction efficiency of 36 % (without energy recovery). The suggested values of the beam energy and the magnetic field for a particular frequency are shown in Fig. 3. A high magnetic field of around 9.5 T is required to excite the operating mode with the highest frequency (244 GHz). The beam energy has to be increased with the frequency (in steps of 0.5 keV) to maintain high interaction efficiency of more than 36 %.

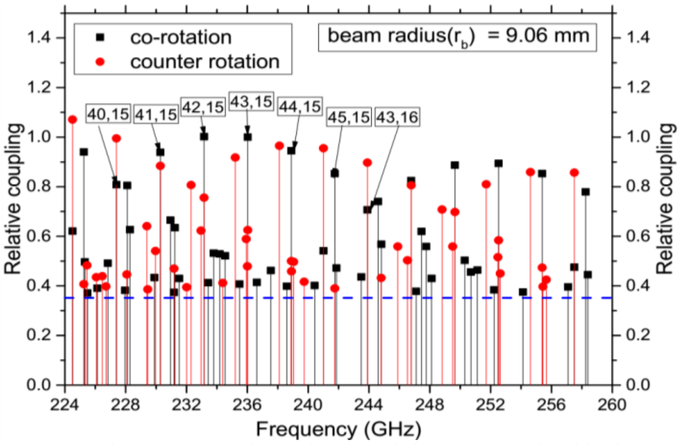

Fig. 1. Mode spectrum in the cavity around the $TE_{43,15}$ mode with electron beam radius of 9.06 mm. The selected modes for frequency tunability have been marked, and are shown along with all neighboring modes having coupling more than 0.35 within −5 % to +10 % of the center frequency.

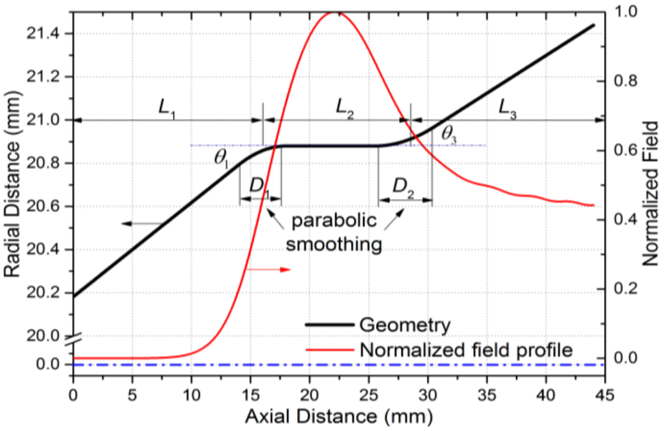

Fig. 2. Hollow-cavity design for the 236 GHz DEMO gyrotron [9].

TABLE III: FINAL PHYSICAL PARAMETERS OF THE 236 GHZ CAVITY.

Cavity radius (R_{cav}) [mm]	Input taper, interaction section and output taper length ($L_1/L_2/L_3$) [mm]	Input and output smoothing length (D_1/D_2) [mm]	Input angle (θ_1)	Output angle (θ_3)
20.88	16/12/16	4/5	2.5°	2°

The cavity wall loading is given by [27],

$$\bar{\rho}_{\text{ohm}} \approx \frac{Q_{\text{diff}} \cdot P_{\text{out}}}{Q_{\Omega} \cdot S} \propto \frac{P_{out} \cdot L_2 \cdot \delta}{\lambda^2 \cdot R_{cav}{}^2 \cdot (1 - m^2/\chi_{m,p}{}^2)} \quad (3)$$

Here, Q_{diff} is the diffractive quality factor, P_{out} is the output power, Q_{Ω} is the ohmic quality factor of cavity, S is the cavity wall area and $\delta = \sqrt{(2 / \sigma\, \omega\, \mu)}$ is the skin depth. With increasing frequency, the diffractive quality factor, output power and the mode eigenvalue increase, while the relative caustic radius (m/χ_{mn}) remains (approximately) constant. These conditions lead to a rise in the wall loading with the operating frequency (see Fig. 4). The starting current calculation has been carried out considering all selected modes for frequency tunability operation and the results are plotted in Fig. 5. At the suggested magnetic field, the starting current of the respective mode is less than the beam current of 43 A. This result demonstrates the possibility of the magnetic tuning, in which the suggested operating modes with the various frequencies (Table I) can be excited by changing the magnetic field.

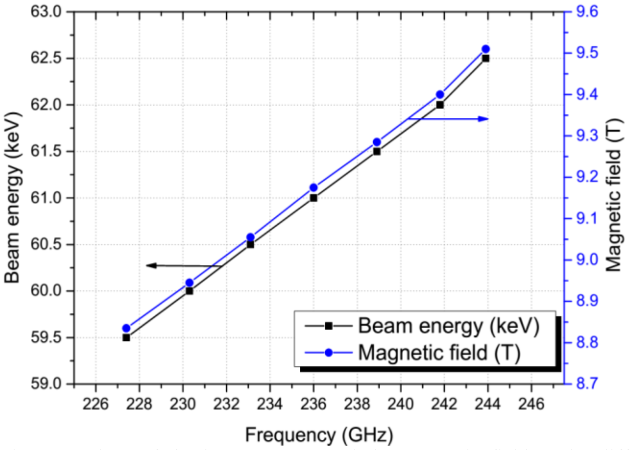

Fig. 3. Values of the beam energy and the magnetic field at the different operating frequencies for a minimum interaction efficiency of 36 % (beam current 43 A).

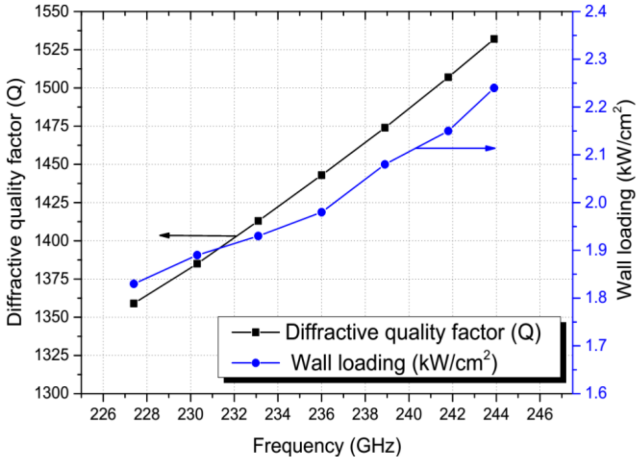

Fig. 4. Diffractive quality factor and wall loading of the cavity at different operating frequencies.

A. Frequency step-tuning: from high frequency to low frequency

The possibility of fast frequency tunability of the DEMO gyrotron has been verified theoretically with the help of time-dependent self-consistent multi-mode simulations (see Fig. 6). The first two plots show the variation of the magnetic field and beam energy over the time, respectively, and the third and fourth plot show the efficiency and output power of the excited mode with consideration of the large number of neighboring modes. The beam energy has been modified at every stage to maintain optimized detuning for sufficiently high efficiency and output power. It is clear from the result that the operating frequency can be easily altered by modifying the magnetic field. Stable RF output of around 1 MW can be achieved at the various operating frequencies and, at least for increasing frequency, in a continuous run. The speed of the frequency tuning is mainly dependent on the rate of the change of magnetic field. As the magnet system for DEMO gyrotron is not finalized yet, so, it is not possible to predict the speed of frequency tunability at this stage.

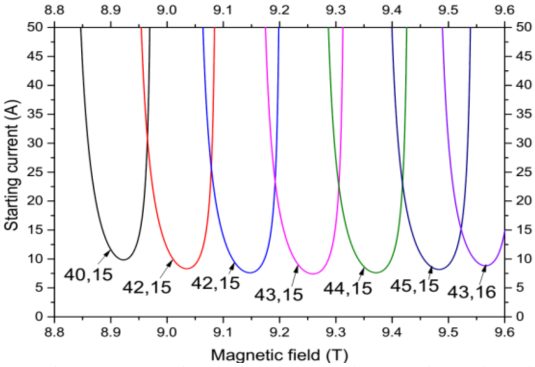

Fig. 5. Starting current plots of the operating modes selected for the frequency tunability. The values of the starting currents are well below the operating current of 43 A for each relevant cavity mode.

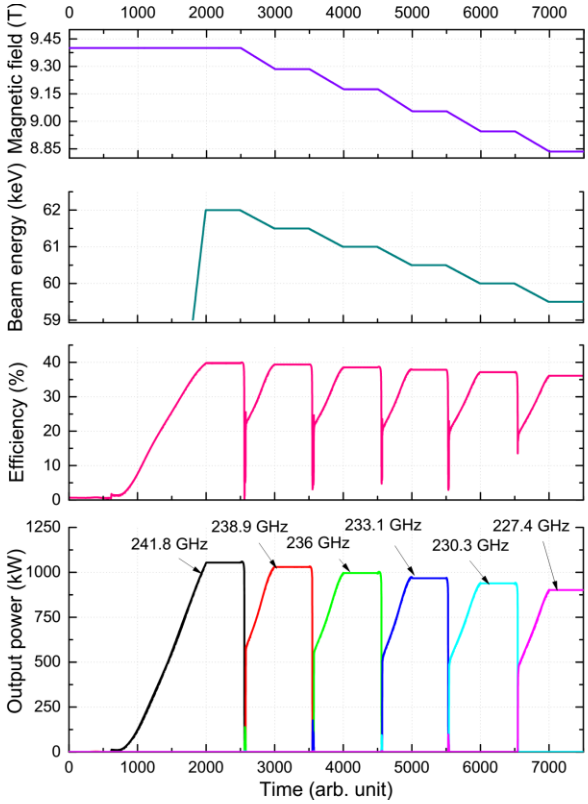

Fig. 6. Step-wise fast-frequency tuning with a changing magnetic field and beam energy. Stable output power (~ 1 MW) with an interaction efficiency of more than 36 % has been achieved at the different operating frequencies.

B. Frequency step-tuning: from low frequency to high frequency

The gyrotron operating frequency is proportional to the magnetic field (from (1)). Unlike the step-frequency tuning from high frequency to low frequency, it is not possible to achieve frequency tunability at the desired 2-3 GHz steps from low frequency to high frequency by simply changing magnetic field, due to hysteresis effects [29]. This case has been studied considering frequency step-tunability from the 236 GHz $TE_{43,15}$ mode to the 238.9 GHz $TE_{44,15}$ mode. In Fig. 7, the output power of both the modes has been plotted at different magnetic fields considering only single mode interaction.

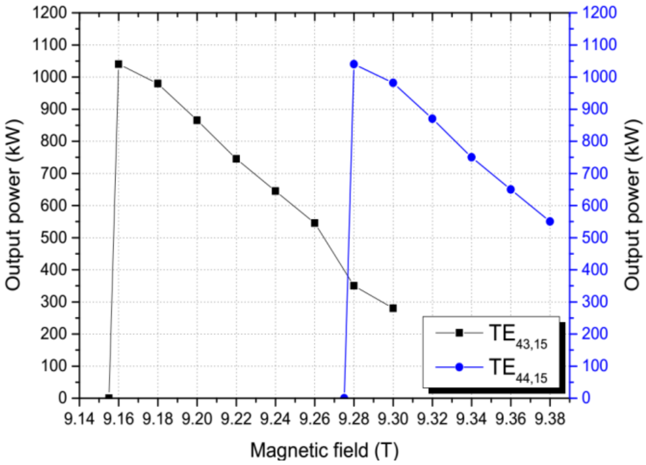

Fig. 7. Output power of the modes $TE_{43,15}$ and $TE_{44,15}$ at different values of the magnetic field. The optimum magnetic field for the $TE_{43,15}$ and $TE_{44,15}$ modes is 9.175 T and 9.285 T, respectively. For the magnetic field higher than the optimum magnetic field, the operating mode remains excited with low detuning and low output power, which prevents the frequency tuning from low frequency to 2-3 GHz higher frequency.

The optimum magnetic field for the excitation of the modes $TE_{43,15}$ and $TE_{44,15}$ with high efficiency is 9.175 T and 9.285 T.In the case of multi-mode time-dependent simulations, when the magnetic field (B_0) has been increased from 9.175 T to 9.285 T, the $TE_{43,15}$ mode remained excited with low detuning and low output power. Since the proposed cavity design is compatible for all suggested frequencies, a possible solution is to reduce the beam energy to low level until the working mode is detuned and then excite the desired mode at the higher frequency by increasing the beam energy again and adjust the magnetic field accordingly (see Fig. 8).

IV. QUASI-OPTICAL LAUCHER DESIGN

For low loss transmission of the output RF wave, the high order cavity mode (TE mode) is converted into a Gaussian like mode using an internal Quasi-Optical mode converter. The mode converter includes an oversized, open-ended slot waveguide (launcher) with the beam-shaping mirrors. The first design of an internal mode converter has been proposed by Vlasov et al. in [30] followed by more advanced designs like

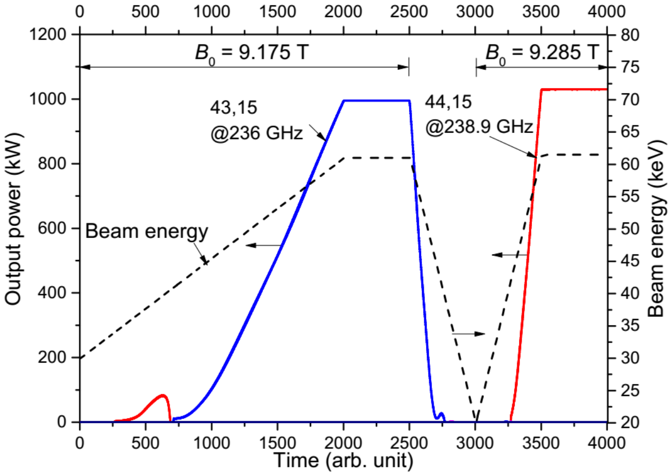

Fig. 8. Frequency step-tuning from low frequency to high frequency by controlling beam energy and magnetic field.

the harmonically deformed launcher [31], the Kirchhoff–Huygens integral equation based mirror-line launcher [32-34] and most recently the hybrid-type launcher, also based on the Helmholtz-Kirchhoff integral theorem [35-36]. The characteristics of the different design approaches are compared in [36] with an overview of the launcher development at KIT.

The harmonically deformed launcher is effective only for cavity modes having a relative caustic radius close to 0.5. In the case of the 236 GHz, $TE_{43,15}$ mode DEMO gyrotron, the relative caustic radius is 0.416. So, the harmonically deformed launcher is not a good choice for high Gaussian mode content and a hybrid-type launcher is selected for this gyrotron. The in-house developed code at KIT for launcher analysis and synthesis (“TWLDO”) is used for the design. The field distribution on the launcher wall of the final design is shown in Fig. 9. The input radius of the launcher is 22.37 mm (corresponding to $1.07 \cdot R_{\mathrm{cav}}$), launcher length and cut length are 227.11 mm and 60 mm, respectively.

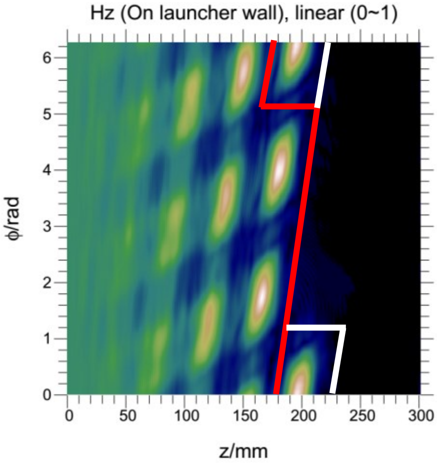

Fig. 9. Field distribution on the hybrid-type launcher wall for the 236 GHz $TE_{43,15}$ mode gyrotron. The edges of the cut and the launcher aperture are indicated in red lines and white line, respectively.

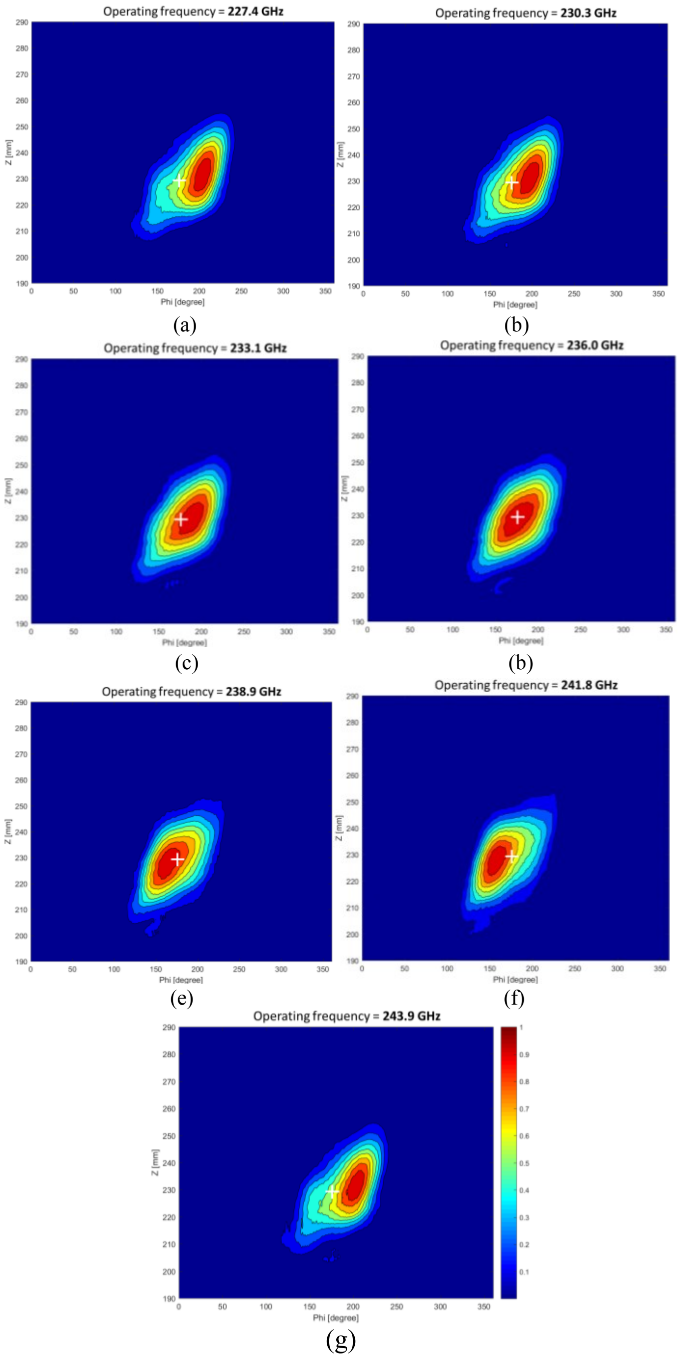

(a) (b) (c) (b) (e) (f) (g)

Fig. 10. Simulated Radiation pattern of the designed launcher at the radial distance of 60 mm using the SURF3D code package for the operating frequencies of: (a) 227.4 GHz, (b) 230.3 GHz, (c) 233.1 GHz, (d) 236.0 GHz, (e) 238.9 GHz, (f) 241.8 GHz, (g) 243.9 GHz, using SURF3D code package at a radial distance of 60 mm. For all radiation plots, x-axis represents azimuthal variation of 0° to 360° and z-axis represents axial distance of 190 mm to 290 mm from launcher start point.

As the relative caustic radii of all selected modes for a step-frequency tunability are close to each other, the performance of the launcher is nearly identical for all selected modes at the various frequencies. The simulated Fundamental Gaussian Mode Content (FGMC) for the different frequencies is listed in Table IV. Using the commercial 3-D full-wave code SURF3D, the radiation pattern of the launcher is calculated for all frequencies at a radial distance of 60 mm (Fig. 10). The field profile is normalized to the maximum value. Compared to the field profile at the frequency of 236 GHz, the RF beam is slightly shifted for the other frequencies due to the small difference in their relative caustic radii, but the overall beam profile remains Gaussian-like with more than 92 % of FGMC. As per the transmission line requirements, the set of focusing mirrors further corrects the beam shape. The design of the beam shaping mirrors is ongoing at KIT.

CONCLUSIONS

In this paper, the possibility of fast frequency tunability in 2-3 GHz steps has been presented for a 236 GHz hollow-cavity DEMO gyrotron. The selection of modes for the frequency-tunable gyrotron is restricted by the requirements that they should have large coupling, suitable frequencies, and their relativistic caustic radius should be nearly identical in order to have the same quasi-optical launcher design for all the selected modes. With the help of realistic numerical simulations, efficient MW-level operation within the ±10 GHz frequency range was demonstrated for the selected modes. The gyrotron operating frequency primarily depends on the operating magnetic field. The speed of frequency tunability is governed by the rate of change in the cavity magnetic field and it is limited by the capabilities of the superconducting gyrotron magnet system. The simulation results support very high conversion efficiency for all selected modes with the designed hybrid-type launcher.

REFERENCES

[1] M. Thumm, “State-of-the-art of high power gyro-devices and free electron maseres, update 2014,” Scientific Report. KIT-SR 7693, Karlsruhe Institute of Technology, Karlsruhe, Germany, 2015.

[2] V. Erckmann, W. Kasparek, B. Plaum, C. Lechte, M. I. Petelin, H. Braune, G. Gantenbein, H.P. Laqua, L. Lubiako, N.B. Marushchenko, G. Michel, Y. Turkin, M. Weissgerber, and the W7-X ECRH-teams at IPP Greifswald, IPF Stuttgart, and KIT, “Large scale CW ECRH systems: some considerations”, EPJ Web of Conferences, vol. 32, 04006, 2012.

[3] T. Omori, M.A. Henderson, F. Albajar, S. Alberti, U. Baruah, T.S. Bigelow, B. Beckett, R. Bertizzolo, T. Bonicelli, A. Bruschi, J.B. Caughman, R. Chavan, S. Cirant, A. Collazos, D. Cox, C. Darbos, M.R. de Baar, G. Denisov, D. Farina, F. Gandini, T. Gassmann, T.P. Goodman, R. Heidinger, J.P. Hogge, S. Illy, O. Jean, J. Jin, K. Kajiwara, W. Kasparek, A. Kasugai, S. Kern, N. Kobayashi, H. Kumric, J.D. Landis, A. Moro, C. Nazare, Y. Oda, I. Pagonakis, B. Piosczyk, P. Platania, B. Plaum, E. Poli, L. Porte, D. Purohit, G. Ramponi, S.L. Rao, D.A. Rasmussen, D.M.S. Ronden, T. Rzesnicki, G. Saibene, K. Sakamoto, F. Sanchez, T. Scherer, M.A. Shapiro, C. Sozzi, P. Spaeh , D. Strauss, O. Sauter, K. Takahashi, R.J. Temkin, M. Thumm , M.Q. Tran, V.S. Udintsev, H. Zohm “Overview of the ITER EC H&CD system and its capabilities”, Fusion Engineering and Design, vol. 86, pp. 951–954, 2011.

[4] M. Thumm, "Recent Advances in the Worldwide Fusion Gyrotron Development," IEEE Transactions on Plasma Science, vol. 42, no. 3, pp. 590-599, 2014.

[5] P. C. Kalaria, M.V. Kartikeyan and M. Thumm, “Design of 170 GHz, 1.5-MW Conventional Cavity Gyrotron for Plasma Heating”, IEEE Transactions on Plasma Science, vol. 42, no. 6, pp.1522–1528, 2014.

[6] G. Federici, R. Kemp, D. Ward, C. Bachmann, T. Franke, S. Gonzalez, C. Lowry, M. Gadomska, J. Harman, B. Meszaros, C. Morlock, F. Romanelli, R. Wenninger, “Overview Of EU DEMO Design and R&D Activities”, Fusion Engineering and Design, vol. 89, no. 7-8, pp. 882–889, 2014.

[7] E. Poli, G. Tardini, H. Zohm, E. Fable, D. Farina, L. Figini, N. B. Marushchenko, L. Porte, "Electron-cyclotron-current-drive Efficiency In DEMO Plasmas", Nuclear Fusion, vol. 53, 013011, 2013.

[8] K. A. Avramides, O. Dumbrajs, S. Kern, I. Gr. Pagonakis, J. L. Vomvoridis," Mode Selection for a 170 GHz, 1 MW Gyrotron", 35th EPS Conference on Plasma Phys., P-4.105, Hersonissos, Greece, 9–13 June 2008.

[9] P. C. Kalaria, A. K. Avramidis, J. Franck, G. Gantenbein, S. Illy, I. Gr. Pagonakis, M. Thumm, J. Jelonnek, "Interaction Circuit Design and RF Behavior of a 236 GHz Gyrotron for DEMO," 9th German Microwave Conference (GeMiC 2015), Nuremberg, Germany, 16–18 March 2015.

[10] R. Wenninger, F. Arbeiter, J. Aubert, L. Aho-Mantila, R. Albanese, R. Ambrosino, C. Angioni, J.-F. Artaud, M. Bernert, E. Fable, A. Fasoli, G. Federici, J. Garcia, G. Giruzzi, F. Jenko, P. Maget, M. Mattei, F. Maviglia, E. Poli, G. Ramogida, C. Reux, M. Schneider, B. Sieglin, F. Villone, M. Wischmeier and H. Zohm, "Advances in the Physics Basis for the European DEMO Design", Nucl. Fusion, vol. 55, 063003, 2015

[11] S. Garavaglia, W. Bin, A. Bruschi, G. Granucci, G. Grossetti, J. Jelonnek, A. Moro, N. Rispoli, D. Strauss, Q. M. Tran, and T. Franke," Preliminary conceptual design of DEMO EC system", AIP Conference Proceedings, vol. 1689, 090009, 2015.

[12] P. C. Kalaria, K. A. Avramidis, J. Franck, S. Illy, I. Gr. Pagonakis, M. Thumm and J. Jelonnek, "Multi-frequency Operation of DEMO Gyrotron with Realistic Electron Beam Parameters," 16th IEEE International Vacuum Electronics Conference (IVEC 2015), Beijing, China, 27-29 April 2015.

[13] V. Igochine, "Active Control of Magneto-hydrodynamic Instabilities in Hot Plasmas", Springer Series on Atomic, Optical and Plasma Physics, 2014. (DOI: 10.1007/978-3-662-44222-7)

[14] R J Buttery, S Gunter, G Giruzzi, T C Hender, D Howell, G Huysmans, R J La Haye, M Maraschek, H Reimerdes, O Sauter, C D Warrick, H R Wilson and H Zohm," Neoclassical Tearing Modes" Plasma Phys. Control. Fusion, vol. 42, 2000.

[15] A. W. Morris," MHD Instability Control, Disruptions, and Error Fields in Tokamaks", Plasma Phy. and Cantrolled Fusion, vol. 34, no.13, pp. 1871-1879, 1992.

[16] F. Felici, J. X. Rossel, G. Canal, S. Coda, B.P. Duval, T.P. Goodman, Y. Martin, J-M. Moret, O. Sauter, D. Testa, and the TCV Team,"Real-time control of multiple MHD instabilities on TCV by ECRH/ECCD", EPJ Web of Conferences, vol. 32, 2005.

[17] H. Zohm and M Thumm, "On the use of step-tuneable gyrotrons in ITER," Journal of Physics: Conference Series, vol. 25, 2005.

[18] M. Thumm, A. Arnold, E. Borie, O. Braz, G. Dammertz, O. Dumbrajs, K. Koppenburg, M. Kuntze, G. Michel and B. Piosczyk, "Frequency step-tunable (114–170 GHz) megawatt gyrotrons for plasma physics applications," Fusion Engineering and Design, vol. 53, Issues 1–4, pp. 407-421, 2001.

[19] J. Franck, A. K. Avramidis, I. Gr. Pagonakis, S. Illy, G. Gantenbeim, M. Thumm and J. Jelonnek, "Multi-Frequency Design of a 2 MW Coaxial-Cavity Gyrotron for DEMO," 40th International Conference on Infrared, Millimeter, and Terahertz waves (IRMMW-THz 2015), Hong Kong, China, 23-28 Aug. 2015.

[20] M. Thumm, A. Arnold, R. Heidinger, M. Rohde, R. Schwab, and R. Spoerl, "Status report on CVD-diamond window development for high power ECRH," Fusion Eng. Des., vol. 53, no. 1, pp. 517–524, 2001.

[21] X. Yang, G. Dammertz, R. Heidinger, K. Koppenburg, F. Leuterer, A. Meier, B. Piosczyk, D. Wagner and M. Thumm,"Design of an ultra-broadband single-disk output window for a frequency step-tunable 1 MW gyrotron," Fusion Eng. Des., vol. 74, pp. 489–493, Nov. 2005.

[22] G. Gantenbein, A. Samartsev, G. Aiello, G. Dammertz, J. Jelonnek, M. Losert, A. Schlaich, T. Scherer, D. Strauss, M. Thumm, D. Wagner, "First Operation of a Step-Frequency Tunable 1-MW Gyrotron With a Diamond Brewster Angle Output Window," IEEE Transactions on Electron Devices, vol.61, no. 6, pp.1806-1811, 2014.

[23] K. A. Avramides, I. Gr. Pagonakis, C. T. Iatrou and J. L. Vomvoridis, "EURIDICE: A code-package for gyrotron interaction simulations and cavity design", 17th Joint Workshop on Electron Cyclotron Emission and Electron Cyclotron Resonance Heating (EC-17), EPJ Web of Conferences, vol. 32, 2012.

[24] S. Kern, "Numerical Codes for interaction calculations in gyrotron cavities at FZK", Proc. 21st Int. Conf. Infrared and Millimeter Waves, Berlin, Invited Paper AF2, 1996; and "Numerische Simulation der Gyrotron-Wechselwirkung" (Numerical simulation of the gyrotron interaction), Scientific Report FZKA 5837, Karlsruhe, 1997.

[25] M. Schmid, J. Franck, P. C. Kalaria, K.A. Avramidis, G. Gantenbein, S. Illy, J. Jelonnek, I. Gr. Pagonakis, T. Rzesnicki and M. Thumm, "Gyrotron development at KIT: FULGOR test facility and gyrotron concepts for DEMO," Fusion Engineering and Design, vol. 96–97, pp. 589-592, 2015.

[26] K. Sakamoto, K. Kajiwara, Y. Oda, K. Hayashi, K. Takahashi, T. Kobayashi and S. Moriyama, "Status of high power gyrotron development in JAEA", 14th IEEE International Vacuum Electronics Conference, Paris, France, 21–23 May 2013.

[27] G. S. Nusinovich, Introduction to the Physics of Gyrotron, The Johns Hopkins University Press, Maryland, 2004.

[28] M. Thumm., J. Franck, P.C. Kalaria, K.A. Avramidis, G. Gantenbein, S. Illy, I.G. Pagonakis, M. Schmid, C. Wu, J. Zhang, J. Jelonnek,"Towards a 0.24-THz, 1-to-2-MW-class gyrotron for DEMO", Terahertz Science and Technology, vol. 8, no. 3, pp. 85-100, 2015.

[29] O. Dumbrajs, T. Idehara, Y. Iwata, S. Mitsudo, I. Ogawa and B. Piosczyk,"Hysteresis-like effects in gyrotron oscillators", Physics of Plasmas, vol. 10, Issue 5, pp. 1183-1186, 2003.

[30] S. N. Vlasov, L. I. Zagryadskaya, and M. I. Petelin, "Transformation of a whispering gallery mode, propagating in a circular waveguide into beam of waves," Radio Eng. Electron Phys., vol. 20, pp. 14–17, 1975.

[31] G. G. Denisov, A. N. Kuftin, V. I. Malygin, N. P. Venediftov, D. V. Vinogradov, and V. E. Zapevalov, "110 GHz gyrotron with built-in high efficiency converter," Int. J. Electron., vol. 72, pp. 1079–1091, 1992.

[32] A. V. Chirkov, G. G. Denisov, M. L. Kulygin, V. I. Malygin, S. A. Malygin, A. B. Pavel'ev, and E. A. Soluyanova, "Use of Huygens' principle for analysis and synthesis of the fields in oversized waveguides", Radiophysics & Quantum Electronics, vol. 49, no. 5, pp. 344-353, 2006.

[33] J. Jin, M. Thumm, B. Piosczyk, S. Kern, J. Flamm and T. Rzesnicki, "Novel Numerical Method for the Analysis and Synthesis of the Fields in Highly Oversized Waveguide Mode Converters", IEEE Transactions on Microwave Theory and Techniques, vol. 57, no. 7, pp. 1661–1668, 2009.

[34] J. Jin, J. Flamm, J. Jelonnek, S. Kern, I. Pagonakis, T. Rzesnicki, and M. Thumm, "High-Efficiency Quasi-Optical Mode Converter for a 1-MW $TE_{32,9}$-Mode Gyrotron", IEEE Transactions On Plasma Science, vol. 41, no. 10, pp. 2748–2753,2013.

[35] J. Jin., G. Gantenbein, J. Jelonnek, and M. Thumm, "A numerical method for the synthesis of highly oversized waveguide mode converters based on the Helmholtz-Kirchhoff integral theorem", to be submitted to IEEE Trans. on Antennas & Propagation for publication.

[36] J. Jin, G. Gantenbein, J. Jelonnek, T. Rzesnicki, and M. Thumm, "Development of Mode Conversion Waveguides at KIT", EPJ Web of Conferences, vol. 87, 04003, 2015.